Submitted to EPRI Workshop on Applications of Chaos, Dec. 1990.

BNL--45178

DE91 001118

Forecasting Catastrophe by Exploiting Chaotic Dynamics*

H.B. Stewart

and

A.N. Lansbury†

Mathematical Sciences Group
Department of Applied Science
Brookhaven National Laboratory
Upton, NY 11973

1. Introduction.

Although chaotic behavior in dynamical systems has sometimes (even by Poincaré [1]) been viewed with dismay, in many instances chaotic dynamics can and should be regarded as presenting opportunities for understanding and for predicting over the short term. From the standpoint of the experimental dynamicist observing the behavior of a system producing a stream of data in the form of a time series, recent studies have used chaotic dynamical time series to examine information content [2], reconstruct multidimensional attractors [3,4], reconstruct vector fields for the purpose of short term forecasting and noise reduction [5,6,7], and find unstable periodic motions [8], which according to Poincaré are the only generally applicable means for understanding structure in phase space.

*This work was supported by the Applied Mathematical Sciences program of the U.S. Department of Energy under Contract No. DE-AC02-76CH00016.

†Permanent address: Department of Civil Engineering, University College, London.

Our purpose here is to introduce a variation on the theme of short term forecasting from a chaotic time series. We show that for the lowest-dimensional chaotic attractors, it is possible to predict incipient catastrophes, or crises, by examining time series data taken near the catastrophic bifurcation threshold, but always remaining on the safe side of the threshold.

More specifically, we assume that some dynamical system has been observed and a time series

$$x_1^1, x_2^1, x_3^1, \ldots x_n^1$$

of the dynamical state variable x at times $j = 1, 2, 3, \ldots n$ has been recorded, and that this dynamical system has a control parameter μ whose value was fixed at μ_1 throughout the observation of the above data. Reconstruction theorems [3] prove that if n is large enough, this single variable time series suffices to generate a complete geometric phase space portrait of the attractor.

Subsequently, with the control at a new fixed setting μ_2, a second time series $\{x_j^2, j = 1, 2, 3, \ldots n\}$ is recorded. This process may be repeated for several values $\mu_i, i = 1, 2, \ldots I$ of the control. Suppose for simplicity that $\mu_1 < \mu_2 < \ldots < \mu_I$. We then ask the following questions: Under what circumstances is it possible to infer that a catastrophic change in dynamical behavior will occur at some critical threshold value μ^* slightly greater than μ_I? Can the threshold value μ^* be estimated from the data recorded for $\mu_i, i = 1, 2, \ldots I$? Our answer is that for dynamical systems with very simple chaotic attractors, this kind of prediction is indeed possible. In other words, chaotic attractors may contain in the record of their behavior sufficient information to predict dynamic catastrophes, without disturbing the dynamics and before any consequences of such a catastrophe can occur.

We consider both a mathematical prototype of chaotic dynamics, the Hénon map, and a more familiar nonlinear oscillator, Duffing's equation with twin-well potential. The behavior of this Duffing oscillator is

important in many applications including structural vibrations [**9**,10], breaking of chemical bonds [**11**], and capsize of ships [**12**]. The method we propose will be applicable to systems having chaotic attractors of lowest possible dimension, that is, slightly greater than one for discrete time dynamical systems. We hope that the ideas presented here may be generalized to higher-dimensional systems, but that will depend in part on better geometric phase space understanding of the possible types of catastrophic bifurcations of chaotic attractors, and in particular the types of unstable basic sets which can collide with attractors to trigger catastrophes [**13**,14,15] or crises [**16**].

2. Catastrophes in the Hénon Map.

The Hénon map is defined by the iteration

$$\begin{aligned} x_{n+1} &= 1 - ax_n^2 + y_n \\ y_{n+1} &= bx_n \end{aligned} \tag{1}$$

of dynamical state variables x and y in a two-dimensional (x, y) phase space. The parameters a and b are the controls of this dynamical system, held at fixed values while equations (1) are iterated from initial conditions (x_0, y_0) to determine the long term behavior. The parameter b is related to the amount of damping or dissipation in the system, with b values close to zero corresponding to strong dissipation; the parameter a may be thought of as a stress parameter, similar to a forcing amplitude in a driven system, with greater a values corresponding to increased forcing or stress. For $b = 0$, equations (1) always give $y_{n+1} = 0$ after the first iteration, so the dynamics are described by the state variable x_n and the one-dimensional map

$$x_{n+1} = 1 - ax_n^2. \tag{2}$$

Equation (2) is an interesting dynamical model in its own right; qualitatively similar modes have found applications in population biology [**17**] and economics [**18**] as well as the physical sciences (e.g. [**19**]).

The dynamical behavior of (2) is by now well known [16,17] and depends in a complicated way on the value of the parameter a. For $a < -\frac{1}{4}$, there is no stable long term behavior, and $x_n \to -\infty$ from every initial condition. For $-\frac{1}{4} < a$ there is an unstable fixed point at $x^* = [-1 - \sqrt{(1+4a)}]/2a$; all initial conditions to the left of x^* diverge to $-\infty$, while for $-\frac{1}{4} < a < 2$ there is an interval of initial conditions to the right of x^* which lead to stable long term behavior, in the sense that iterates remarks bounded for all time. For $-\frac{1}{4} < a < \frac{3}{4}$ the stable behavior is a fixed point; increasing the stress parameter a beyond $\frac{3}{4}$, the stable long term behavior bifurcates by successive period doubling and becomes chaotic. There are many small intervals of a values for which the unique stable behavior is periodic, repeating exactly after p iterates. As a approaches 2 these windows of periodic behavior become narrower, and chaotic dynamics predominate: iterates wander over an interval of x values, and there is sensitive dependence on initial conditions, so that nearby initial conditions separate under iteration at an exponential rate.

At $a = 2$, the stress reaches a critical value and a catastrophe occurs: the interval of x values visited by long term iterates (in other words, the chaotic attractor) touches the unstable fixed point x^*. For any $a > 2$, chaotic motions can not be sustained, and there is no stable long term behavior. This loss of stability of the chaotic attractor which existed for $a < 2$ is associated with the attractor touching x^* at $a = 2$, and is an example of a blue sky catastrophe [14], or boundary crisis [16].

The behavior of equation (2) near $a = 2$ is illustrated in Figure 1, where successive iterates are plotted showing x_{n+1} versus x_n. The heavy dots are 1000 long term iterates computed from (2) after discarding the first 500 iterates. The dashed curve shows the locus of $f(x) = 1 - ax^2$; this locus intersects the 45° line $f(x) = x$ in two points, the leftmost being the unstable separator x^*, marked by a small circle.

Comparison of the two cases $a = 1.95$ and $a = 1.99$ in Figure 1 shows that the left edge of the attractor moves closer to x^* as the control

a approaches 2. For the one-dimensional map (2) the left edge of a chaotic attractor is the second image of the critical point $x = 0$, that is $f(f(0)) = f(1) = 1 - a$. (We ignore the small intervals of a values for which the attractor is periodic.) It will be convenient to measure the distance from this point to x^* vertically in Figure 1; by this measure the distance $D(a)$ is

$$D(a) \equiv f(1-a) - x^* = 1 - a(1-a)^2 - [-1 - \sqrt{(1+4a)}]/2a \qquad (3)$$

which is a continuous function of a for $a > 0$ and goes to zero as $a \to 2$.

Because this distance varies smoothly with a, we might use $D(a)$ as measure of how close the system is to the catastrophe at $a = 2$. Suppose for example that the data represented by heavy dots in Figure 1 were obtained from observation of a black box dynamical system at two different control settings a_1 and a_2. In this situation the broken curve representing $f(x)$ is not known. Nevertheless, we observe that the left edge of the attractor is close to the 45° line, or bisectrix, where $x_{n+1} = x_n$. Furthermore, we note that whatever $f(x)$ may be, it certainly has slope greater that 1 near the left edge of the attractor; therefore when the attractor edge reaches the bisectrix, the contact point must be an unstable separator. This implies that a crisis will occur, although we cannot in general say whether the attractor will explode (interior crisis) or lose stability altogether (boundary crisis). In any case $D(a_1)$ and $D(a_2)$ can be estimated by extending the attractor locus to the bisectrix (by linear extrapolation, for example) to estimate the location of the unstable separator $x^*(a_1)$ and $x^*(a_2)$. Once $D(a_1)$ and $D(a_2)$ are estimated in this way, it is a simple matter to estimate by extrapolation the critical value a^* for which $D(a^*) = 0$. Thus by exploiting the simple chaotic structure of the dynamics and using the fact that any fixed point must lie on the bisectrix in an (x_n, x_{n+1}) plot, we can predict an incipient catastrophe.

In order for this forecasting method to be useful, two remaining obstacles must be overcome. The first is that for the Hénon map with $b \neq 0$, and for Poincaré maps of forced oscillators such as the Duffing

oscillator, the distance from attractor edge to the separator point is not a continuous function of a generic control. Since there are no closed form expressions for this distance generalizing (3), we shall turn to numerical evidence. In so doing we shall also obtain information about the second obstacle, which is that the unstable separator point may in general not be a fixed point, but can instead be a periodic point with period $p > 1$.

The dynamical behavior of the Hénon map for $b < 0$, and also the typical behavior of many simple dynamical systems like nonlinear oscillators, resembles the quadratic map in many ways. There is period doubling leading to chaos as the stress parameter a is increased with b fixed; small windows of a values in the chaotic regime can be found where only periodic attractors exist. And at some threshold $a^* = a^*(b)$, the main attractor loses stability, and for $a > a^*(b)$ all orbits diverge to infinity. (In oscillators, the system would not diverge but would typically jump to a different attractor representing qualitatively different behavior, as in the familiar jump to resonance [20].) The principal difference from the quadratic map is that more than one attractor may coexist for certain values of $a < a^*(b)$.

For $b < 0$ the Hénon map has two fixed points

$$x^* = \{(b-1) - \sqrt{[(b-1)^2 + 4a]}\}/2a \tag{4}$$
$$y^* = bx^*$$

and

$$\bar{x} = \{(b-1) + \sqrt{[(b-1)^2 + 4a]}\}/2a \tag{5}$$
$$\bar{y} = b\bar{x}.$$

By linearizing the Hénon map near (x^*, y^*), the eigenvectors and eigenvalues, or multipliers, can be computed. One multiplier is greater than one, and both are positive, so (x^*, y^*) is an unstable saddle separator, analogous to x^* with $b = 0$. Likewise $(\bar{x}, \bar{y})$ is found to be (after the

first period doubling) unstable with negative multipliers, analogous to the point in Figure 1 where $1 - ax^2$ crosses the bisectrix with negative slope.

In cases where more than one attractor exists, numerical simulations usually show one large chaotic attractor containing $(\bar{x}, \bar{y})$ which attracts most initial conditions; and periodic or small chaotic attractors with much smaller basins of attraction. We concentrate attention on this large attractor, which we call the main attractor, and determine $a^*(b)$ by the following numerical experiment. First we fix b at $b = -0.0001$, and $a = 1.5$. An orbit is started at $(x_0, y_0) = (x_0, bx_0)$ where $x_0 = \bar{x} + .0001$ and iterated 50,000 times. If the result stays to the right of (x^*, y^*) we consider that a^* has not been reached, increase a to 2.0, and check that the resulting orbit diverges within 50,000 iterates. We then conduct a binary search for two a values between 1.5 and 2.0, separated by less than 10^{-5}, such that the orbit started at (x_0, y_0) remains bounded for the smaller a and diverges for the larger a. This gives $a^* = a^*(b = -0.0001)$. We then increment b by -0.0001 and search again for $a^*(b)$.

The results of this experiment are shown in Figure 2. A point is plotted at $a^*(b)$ for each trial b value, and with a very few exceptions these dots fall on an arc emerging from $b = 0, a^*(0) = 2$. Further examination shows that as $a \to a^*(b)$, the main chaotic attractor just touches the saddle fixed point $(x^* y^*)$, and loses stability in a boundary crisis, or blue sky catastrophe. This holds true for $0 > b \gtrsim -0.08$, where $a^*(b)$ turns a corner in Figure 2.

A second experiment was then performed to measure the distance from attractor to (x^*, y^*) for $1.5 < a < a^*(b)$. The results are shown in Figure 3. Here the dashed arc represents the distance $D(a)$ for $b = 0$ computed from equation (3), again ignoring the small regimes of periodic attractors; the heavy arcs consist of numerically determined distances from (x^*, y^*) to the main attractor. These distances were found by using equation (4) for (x^*, y^*) and taking the closest iterate (x_n, y_n),

$1000 < n < 6000$. One technical detail should be noted: only iterates (x_n, y_n) with $y_n > 0$ are tested for closeness to (x^*, y^*); iterates with $y_n < 0$ may be closer to (x^*, y^*) if $a \ll a^*$, but should not be counted because they correspond to points on the right half of the quadratic map, and would be very far from (x^*, y^*) if the y coordinate were rescaled.

Figure 3 shows that the observed distance does go to zero in every case except $b = -0.09$. To exploit the distance as a predictor, we would like the heavy arcs in Figure 3 to be free of discontinuities. In fact they are not; two types of discontinuities are apparent. The first type is rare isolated dots lying above the general trend; this is due to small windows of a values where the main chaotic attractor collapses to a stable periodic orbit. This type of discontinuity occurs even for $b = 0$, and would be easily recognized in experiments, since the general trends on either side of such windows are nearly identical; in real dynamical systems with parametric noise such discontinuities would be entirely suppressed.

A second kind of discontinuity is an apparent step jump in distance; caused by a sudden increase in size of the main attractor, that is, an attractor explosion or interior crisis. For each value $b = -0.01$, -0.03, -0.05, and -0.07 one large jump occurs, and any attempt to predict a^* using values of a to the left of this jump would be doomed to failure. This large jump is caused by an unstable period 3 orbit touching the chaotic attractor to trigger explosion; this explosion occurs along the dashed arc in Figure 2 emerging from the period 3 window of the quadratic map bifurcation diagram at $b = 0, a \simeq 1.75$.

Mathematical theory suggests that there are in fact infinitely many additional attractor explosions causing jumps in the distance to (x^*, y^*). But examination of Figure 3 shows only a very few jumps of much smaller magnitude. This suggests that in practice prediction of a^* is feasible if only the large jump can be taken into account. This is indeed possible, as we shall see shortly.

3. Forecasting catastrophe.

Let us now return to the viewpoint discussed at the beginning, namely that of an experimental dynamicist presented with only time series data recorded from a black box dynamical system; we assume that more than one time series has been recorded, each at a different know value of μ_i of some control parameter. We emphasize that the dynamicist knows only the values of the μ_i and the corresponding data $\{x_j^i\}$, and desires to estimate the critical value $\mu^* > \mu_I$ at which a catastrophic change in the attractor will occur.

To apply distance to the unstable saddle as a practical predictor, it remains to find some means of locating this saddle using only such information as would be available in an experimental observation, namely a sequence of data $\{x_j^i\}$ on the attractor. Our strategy is to use μ values near μ^*, where many of the $\{x_j^i\}$ data correspond to points close to the unstable saddle. In general, this provides an opportunity to reconstruct dynamical rules (for example following [5]) and use the reconstructed rules to estimate the location of the unstable saddle by extrapolation. Here we choose instead to use an equivalent graphic device based on the simple structure of the chaotic attractor, and motivated by Figure 1.

To demonstrate this we turn for our example to the forced Duffing oscillator

$$\ddot{x} + k\dot{x} - x + x^3 = A\sin\omega t \tag{6}$$

which describes damped, forced oscillations of system in a twin-well potential $v(x) = -x^2/2 + x^4/4$. This has been invoked as a model for mechanical vibrations of a vertical Euler support column loaded past the buckling point and shaken laterally [9]. We consider a region of the (ω, A, k) parameter space where nonlinear resonance produces two coexisting attractors in each potential well; this well-known phenomenon (see e.g. [20]) has recently been shown to play an important role in the escape from confinement within a generic potential well with smooth potential barrier [21], having a wide range of applications from the breaking of

molecular bonds [11] to the capsize of ships [12]. Typically in such situations the resonant motion becomes chaotic just before losing stability, and the chaotic attractor bears a very strong resemblance to the attractors of the Hénon map. It is this destabilization of the resonant chaotic motion which we aim to forecast.

Figure 4 shows 100 data points from each of two time series $\{x_j^1\}$ and $\{x_j^2\}$ computed from equation (6) with $k = 0.5, \omega = 0.9$, and $A_1 = 0.348$ for the first series, $A_2 = 0.350$ for the second series. The points are sampled stroboscopically at $t = 2\pi n, n = 1, 2 \ldots$ Treating these as data from a black box dynamical system, we might infer from the slightly greater range of x values in the second case that it is under somewhat greater stress than the first case. However, it seems impossible to guess from this traditional presentation of the data whether the system is near a critical threshold of catastrophic change.

Figure 5 shows the same time series (extended to 500 points each) presented as plots of x_{n+1} versus x_n. Here we see clearly that the second case has a fingertip of the attractor very close to the first bisectrix or 45° line, and we infer that some sort of catastrophe is imminent. In fact a very small increase in A of less than .0002 causes the attractor to lose stability, with an ensuing rapid transient jump to another attractor, in this case the nonresonant periodic motion which oscillates with a much lesser response amplitude measured from the bottom of the potential well.

As an example of forecasting by extrapolation, we consider another set of parameter values, illustrated in Figure 6 showing 500 points on a resonant motion of equation (6) with $k = 0.35, \omega = 1$, and $A = 0.260$ (a) as well as $A = 0.261$ (b). The points are sampled stroboscopically at $t = 2\pi n, n = 1, 2, \ldots$ and plotted x_{n+1} vs. x_n, with the bisectrix drawn. By comparing the two cases, we see that an attractor tip (with slope > 1) is moving toward the bisectrix near $x_{n+1} = x_n \simeq 0.5$. In each case we estimate by linear extrapolation from the tip to the point

where the attractor will touch the bisectrix, and the distance from that point to the attractor tip. Comparing the distances obtained in the two cases, we estimate that the attractor will touch the bisectrix when $A = .2618$. In fact, numerical experiments show the attractor losing stability between $A = .2616$ and $A = .2617$, with an ensuing jump back to the non-resonant periodic motion.

It happens in this example that A values less than 0.260 are not useful because the attractor undergoes a substantial explosion in size at $A \simeq 0.2595$. As with the Hénon map, this explosion is triggered when the chaotic attractor touches an unstable periodic orbit of period 3. Thus to forecast the ultimate loss of stability correctly, we would need forewarning of this explosion. This can be achieved by plotting x_{n+3} versus x_n, as illustrated in Figure 6(c) with $A = 0.259$. Here we see the rightmost tip of the attractor near the bisectrix; by increasing A we could observe this tip moving closer and just touching the bisectrix when the attractor explodes.

Note that forecasting does not predict the outcome of the catastrophe, which as just shown might be either an attractor explosion or a complete loss of stability, i.e. a blue sky catastrophe. To further illustrate this point, Figure 6(d) shows attractor points of equation (6) with $k = 0.25$, $\omega = 1$, and $A = 0.192$. As in Figure 6(c), the attractor is approaching the bisectrix plotted x_{n+3} vs. x_n. But in this case, upon touching the implied period 3 unstable orbit, the chaotic attractor will undergo a blue sky catastrophe, not an explosion as in Figure 6(c). Indeed Figure 6(d) is a preview of a catastrophe studied earlier in [**23**].

Finally, we note that the simple graphical device of Figures 5 and 6 works because the attractor has a simple, thin shape which is well approximated by a curve due to the extreme compression of fractal layers. In more general systems, this graphical device might not be applicable, but the underlying principle would still be valid: a chaotic attractor near incipient catastrophe is close in phase space to some singularity

representing instability, and the distance from attractor to singularity can be estimated from the information contained in the data observable from dynamics on the attractor.

4. Conclusions.

To summarize, we have shown that it is possible in simple dynamical systems to predict an incipient catastrophic change in dynamical behavior using only observed experimental data taken before the catastrophe. The prediction does not specify what form the post-catastrophe behavior will take. Also it is useful to know the period of the unstable motion suspected of triggering the catastrophe; in our examples, the period was either 1 or 3. Mathematical theory suggests that this forecasting procedure might be disrupted by numerous attractor explosions, but in practice these disruptions can to a first approximation be ignored, at least for the Hénon map attractor which is the most commonly observed chaotic attractor in simple dynamical systems. Thus the record of information observable from a chaotic dynamical system may be sufficient to forecast catastrophe.

The authors thank Michael Thompson, Kurt Wiesenfeld, and Ralph Abraham for stimulating discussions. We are grateful to Charles A. Norton for automating the computation of Figures 2 and 3, and to the Science and Engineering Research Semester Program of the U.S. Department of Energy for supporting us. H.B.S. acknowledges the support of the Department of Energy's Applied Mathematical Sciences program. A.N.L. acknowledges a travel grant from the Royal Society of London.

List of Figures

REFERENCES

1. H. Poincaré, "Les méthodes nouvelles de la mécanique céleste," Gauthier-Villars, Paris, 1899.
2. R. Shaw, *Strange attractors, chaotic behavior, and information flow*, Z. Naturf. **36a** (1981), 80–112.
3. F. Takens, *Detecting strange attractors in turbulence*, in "Dynamical Systems and Turbulence," Springer-Verlag, New York, 1980.
4. N.H. Packard, J.P. Crutchfield, J.D. Farmer, and R. Shaw, *Geometry from a time series*, Phys. Rev. Lett. **45** (1980), 712–716.
5. J.D. Farmer and J.J. Sidorowich, *Exploiting chaos to predict the future and reduce noise*, preprint, (1988).
6. J.P. Crutchfield and B.S. McNamara, *Equations of motion from a data series*, Complex Systems **1** (1987), 417–452.
7. J. Cremers and A. Hübler, *Construction of differential equations from experimental data*, Z. Naturf. **42a** (1987), 797–802.
8. D. Auerbach, P. Cvitanovic, J.-P. Eckmann, G. Gunaratne, and I. Procaccia, *Exploring chaotic motion through periodic orbits*, Phys. Rev. Lett. **58** (1987), 2387–2389.
9. F.C. Moon and P.J. Holmes, *A magnetoelastic strange attractor*, J. Sound Vib. **65** (1979), 285–296.
10. P.J. Holmes, *A nonlinear oscillator with a strange attractor*, Phil. Trans. Roy. Soc. A **292** (1979), 419–448.
11. N. Bloembergen, *Comments on the dissociation of polyatomic molecules by intense* $10.6\mu m$ *radiation*, Optics Commun. **15** (1975), 416–418.
12. J.M.T. Thompson, R.C.T. Rainey, and M.S. Soliman, *Ship stability criteria based on chaotic transients from incursive fractals*, Phil. Trans. Roy. Soc. A **332** (1990), 149–167.
13. E.C. Zeeman, *Bifurcation and catastrophe theory*, in "Papers in Algebra, Analysis, and Statistics," Amer. Math. Soc., Providence, RI, 1982.
14. R.H. Abraham, *Chaostrophes, intermittency, and noise*, in "Chaos, Fractals, and Dynamics," Dekker, New York, 1985.
15. H.B. Stewart and J.M.T. Thompson, *Towards a classification of generic bifurcations in dissipative dynamical systems*, Dyn. Stab. Systems **1** (1986), 87–96.
16. C. Grebogi, E. Ott, and J.A. Yorke, *Crises, sudden changes in chaotic attractors, and transient chaos*, Physica D **7** ((1983)), 181–200.
17. R.M. May, *Simple mathematical models with very complicated dynamics*, Nature **261** (1976), 459–467.
18. R.H. Day, *Irregular growth cycles*, Amer. Econ. Rev. **72** (1982), 406–414.
19. R. Shaw, "The Dripping Faucet as a Model Chaotic System," Aerial Press, Sant Cruz, CA, 1984.
20. A.H. Nayfeh and D.T. Mook, "Nonlinear Oscillations," Wiley, New York, 1979.
21. J.M.T. Thompson, *Chaotic phenomena triggering escape from a potential well*, Proc. Roy. Soc. A **421** (1989), 195–225.

Fig. 1a

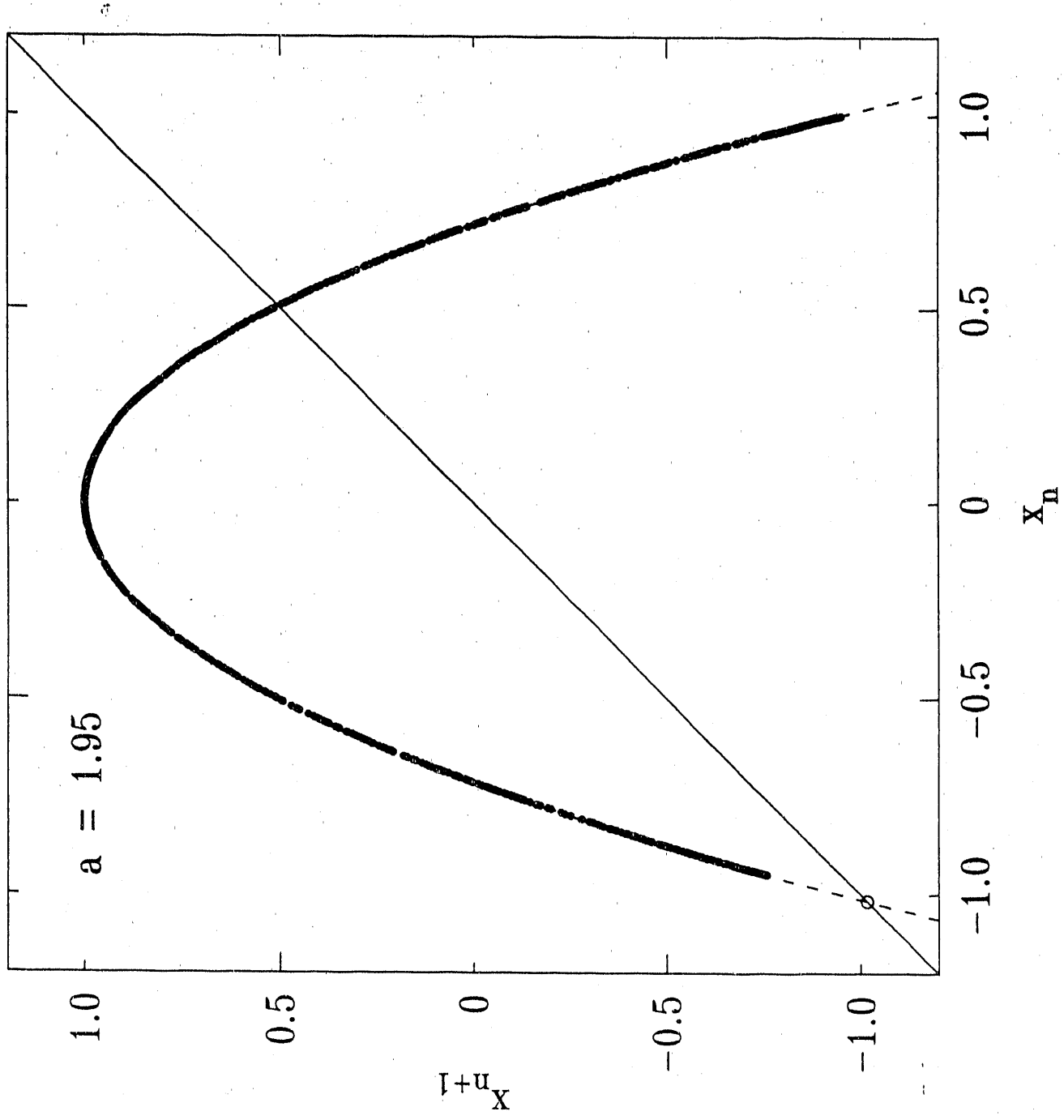

Fig. 1b

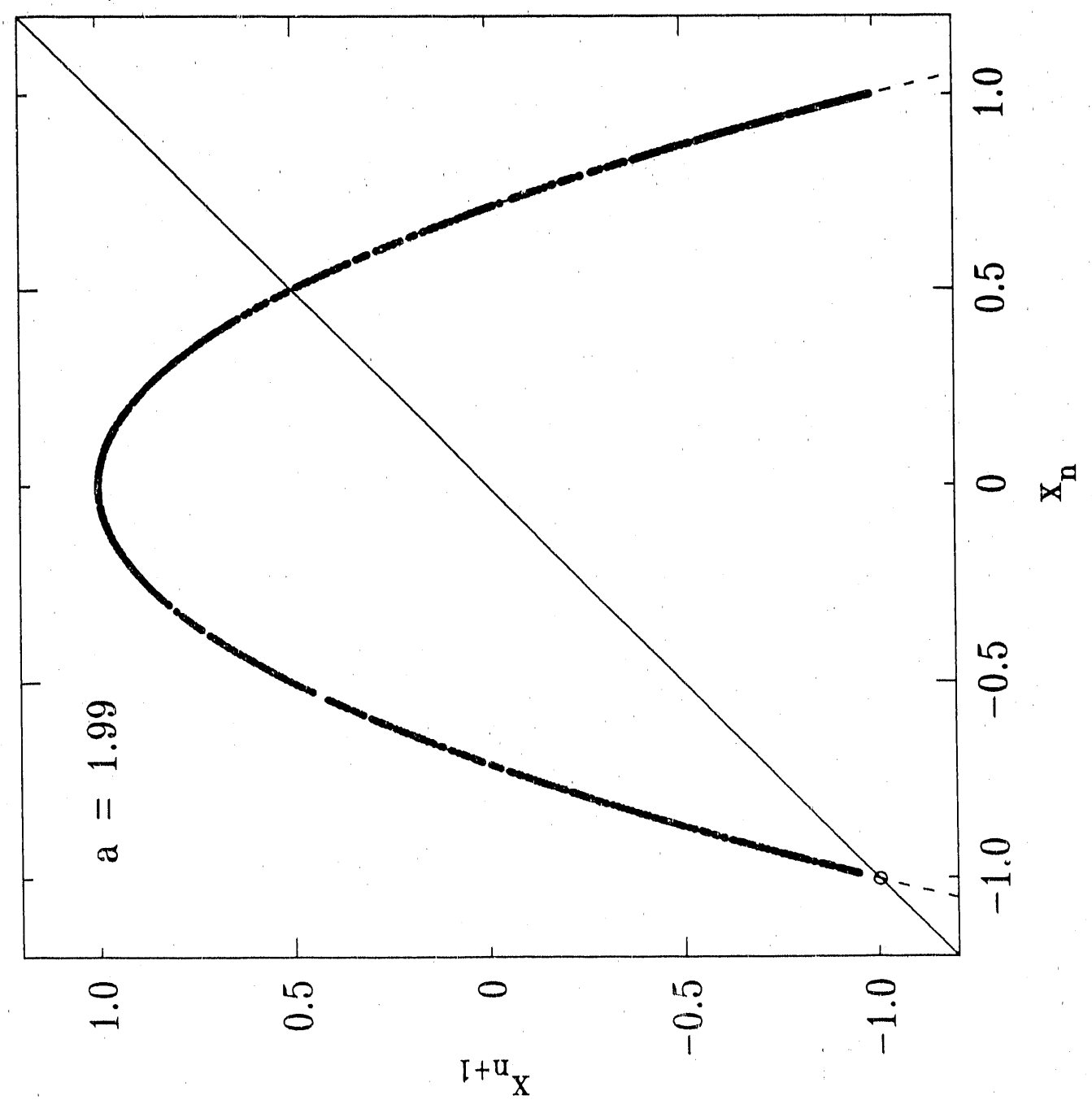

Fig. 2

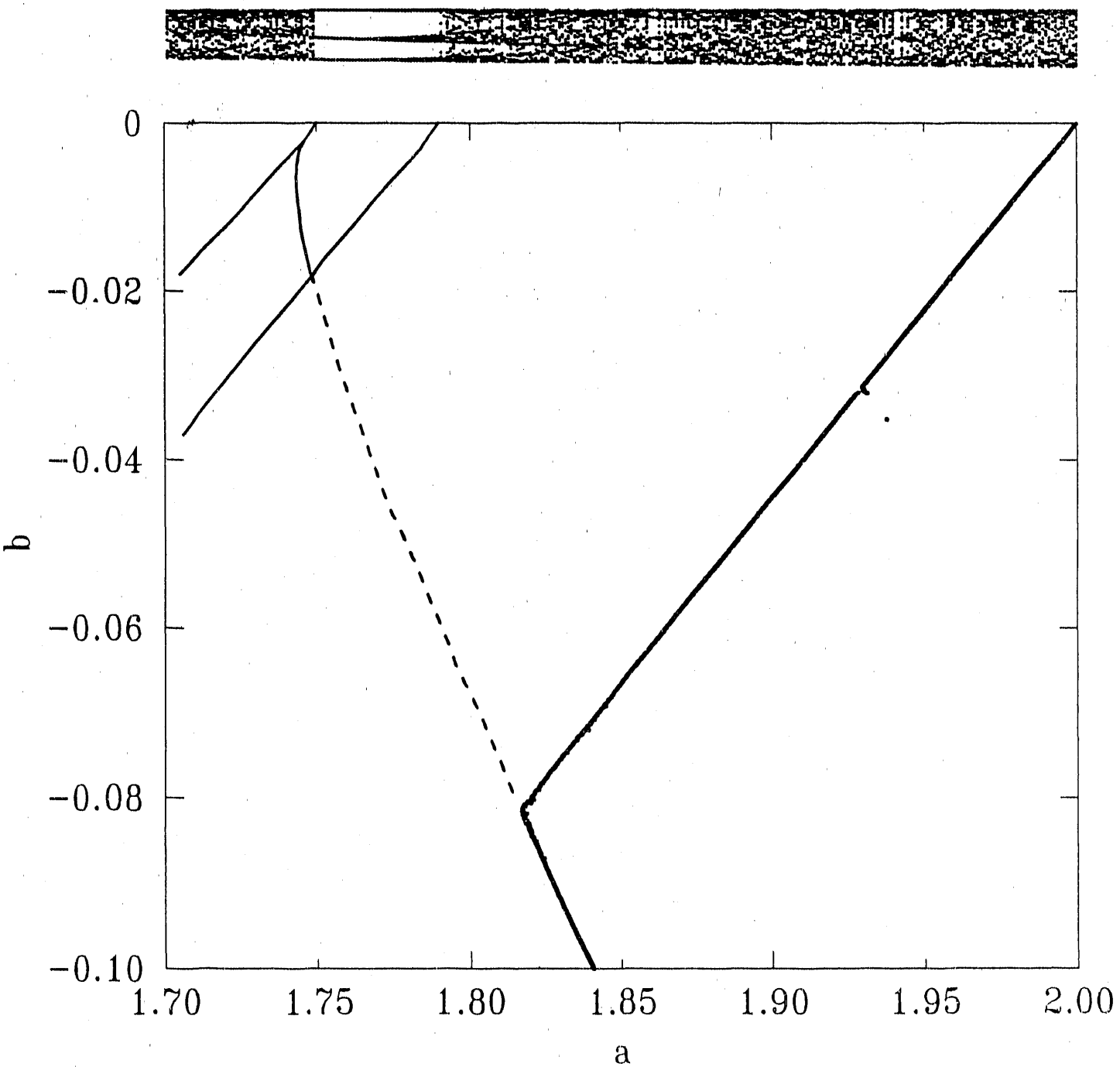

Fig. 3

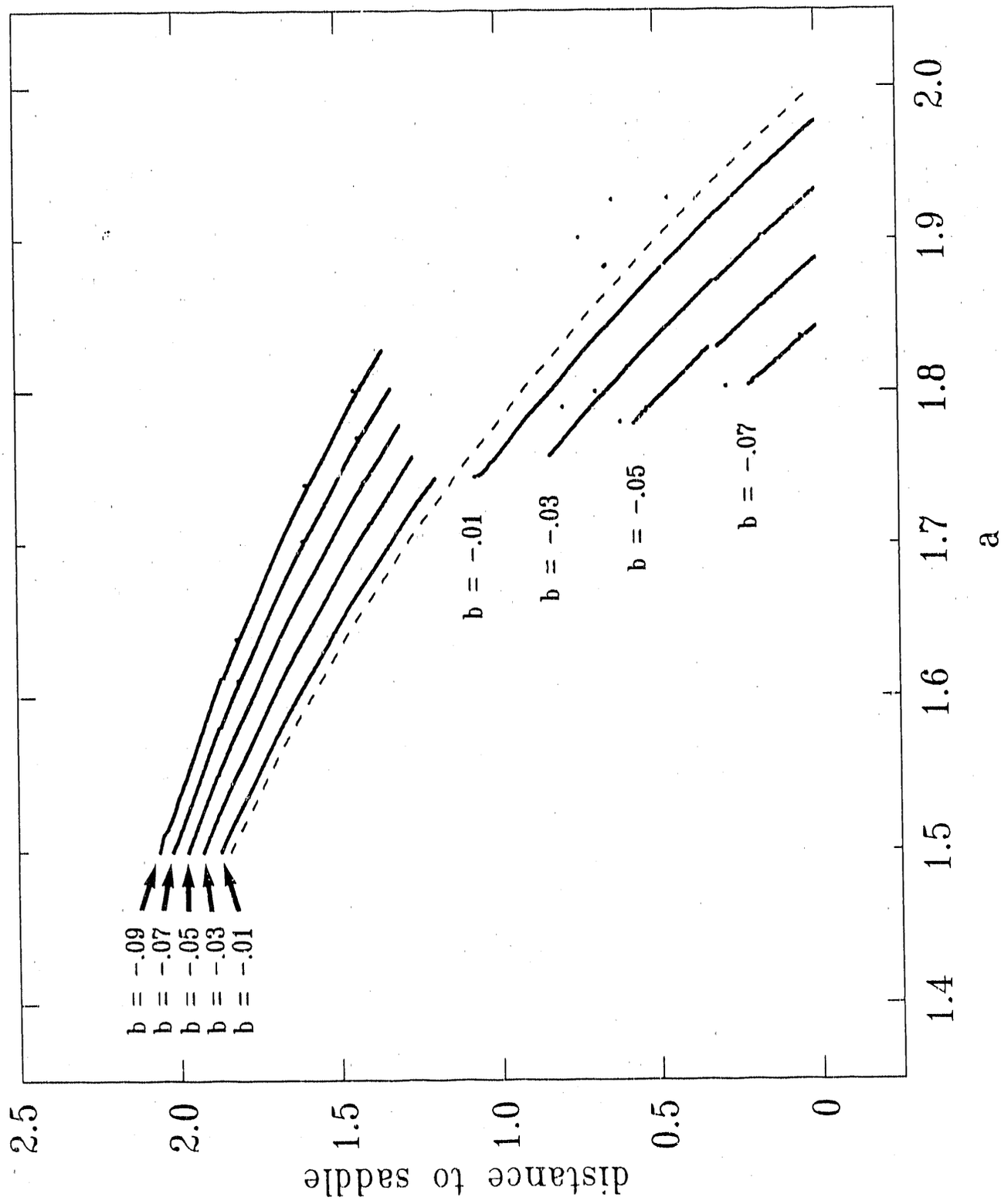
distance to saddle
2.5
2.0
1.5
1.0
0.5
0
1.4
1.5
1.6
1.7
1.8
1.9
2.0
a
b = −.09
b = −.07
b = −.05
b = −.03
b = −.01
b = −.01
b = −.03
b = −.05
b = −.07

Fig. 4

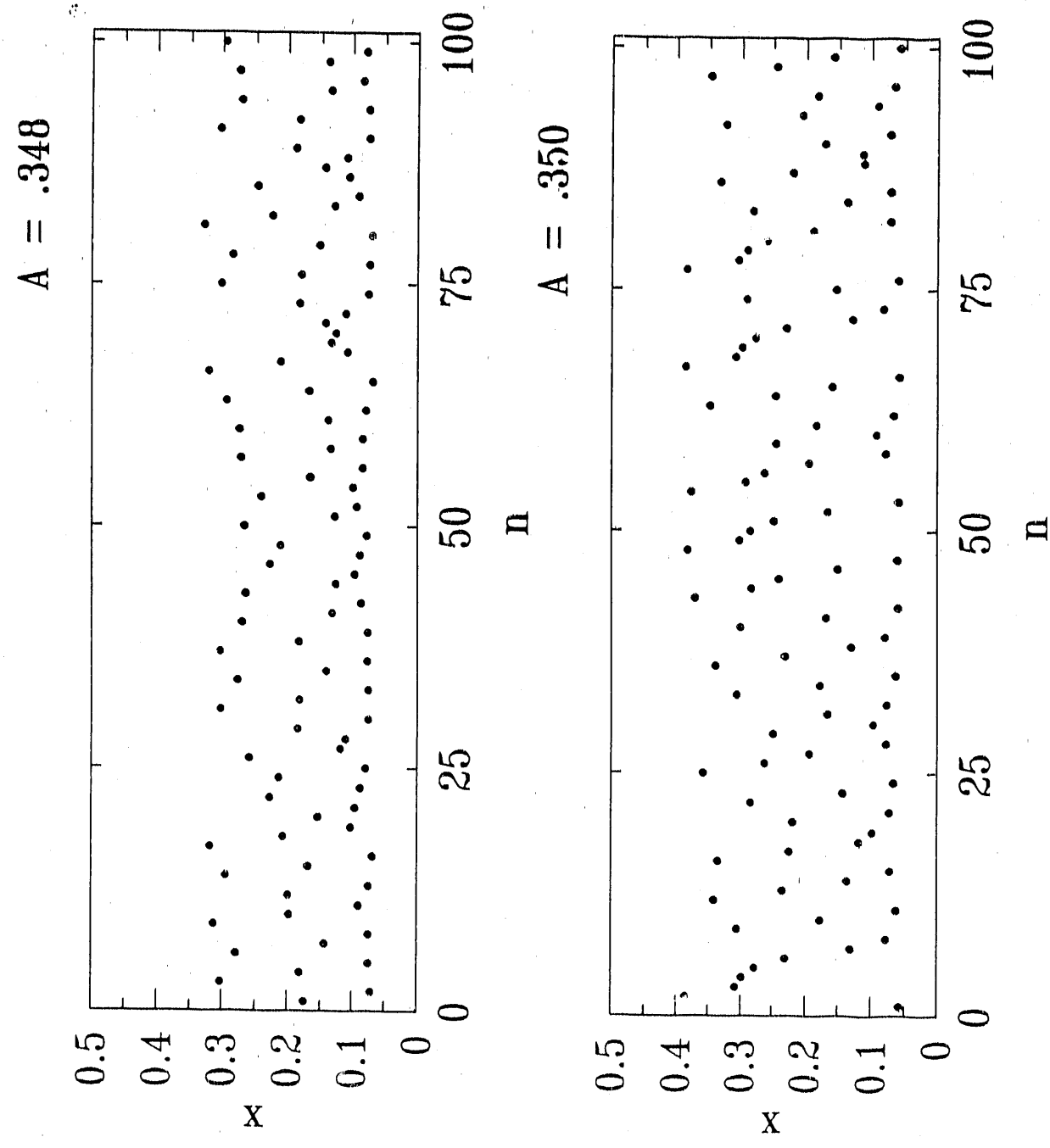

Fig. 5a

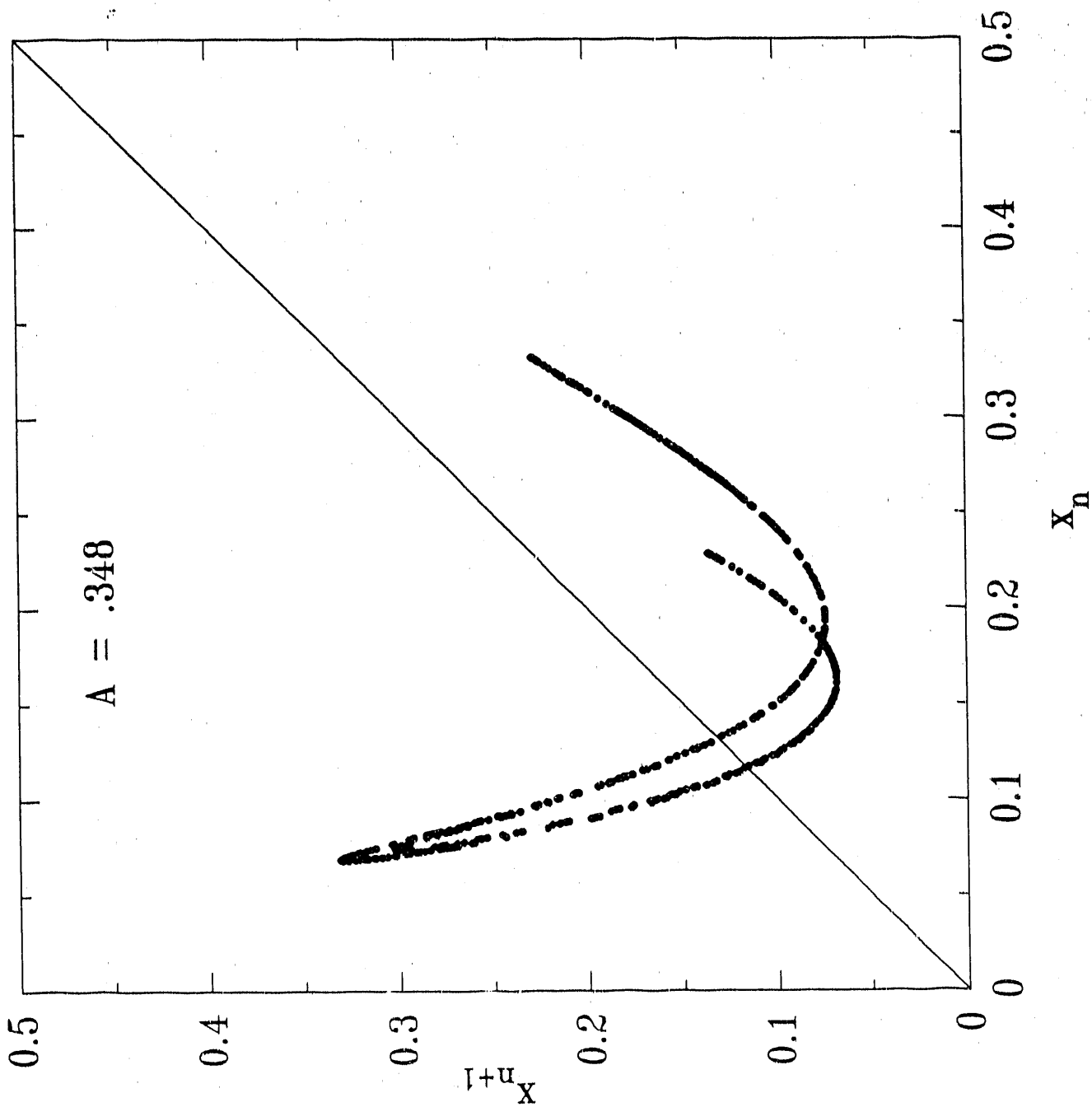

Fig. 5b

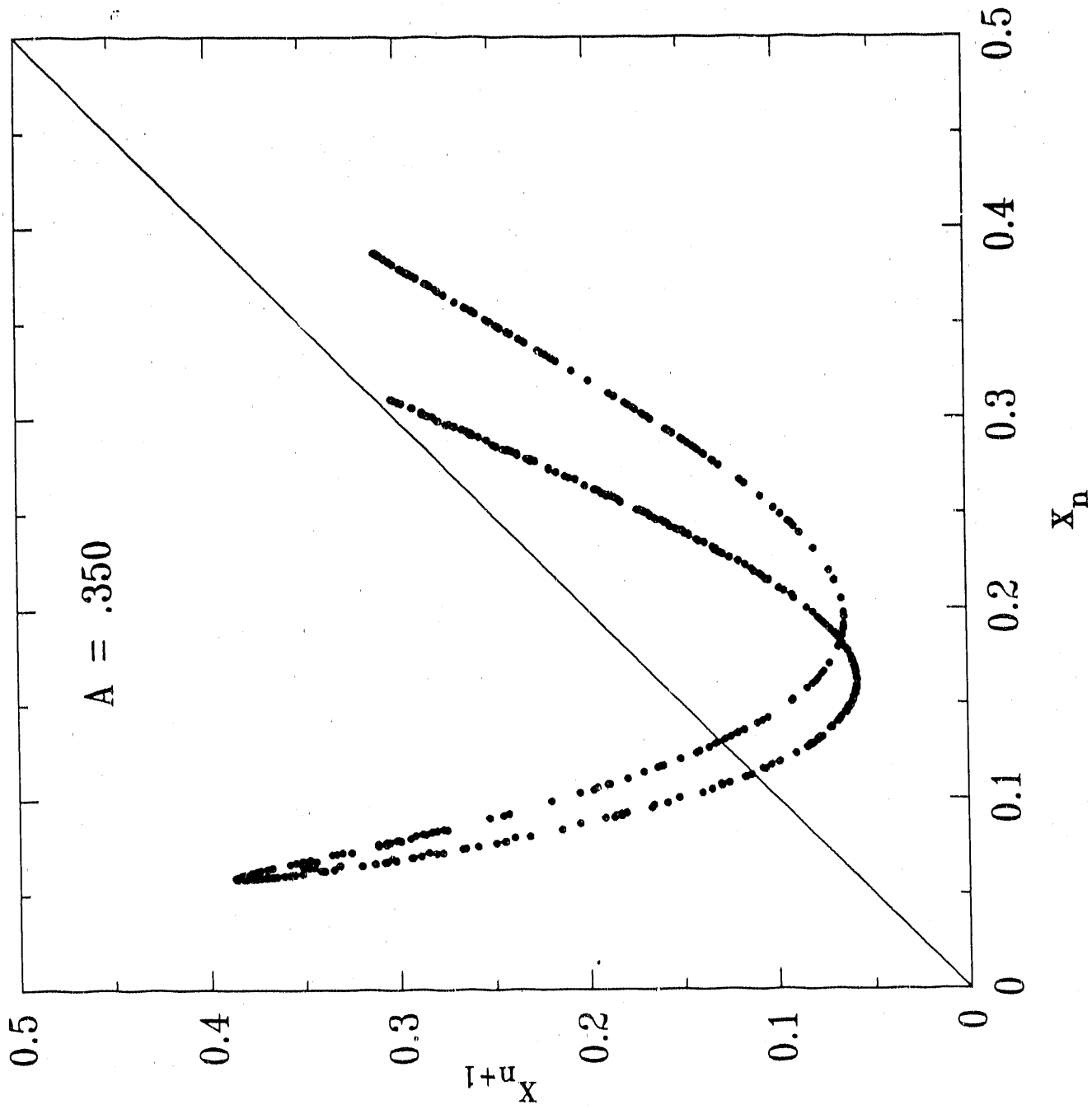

Fig. 6a

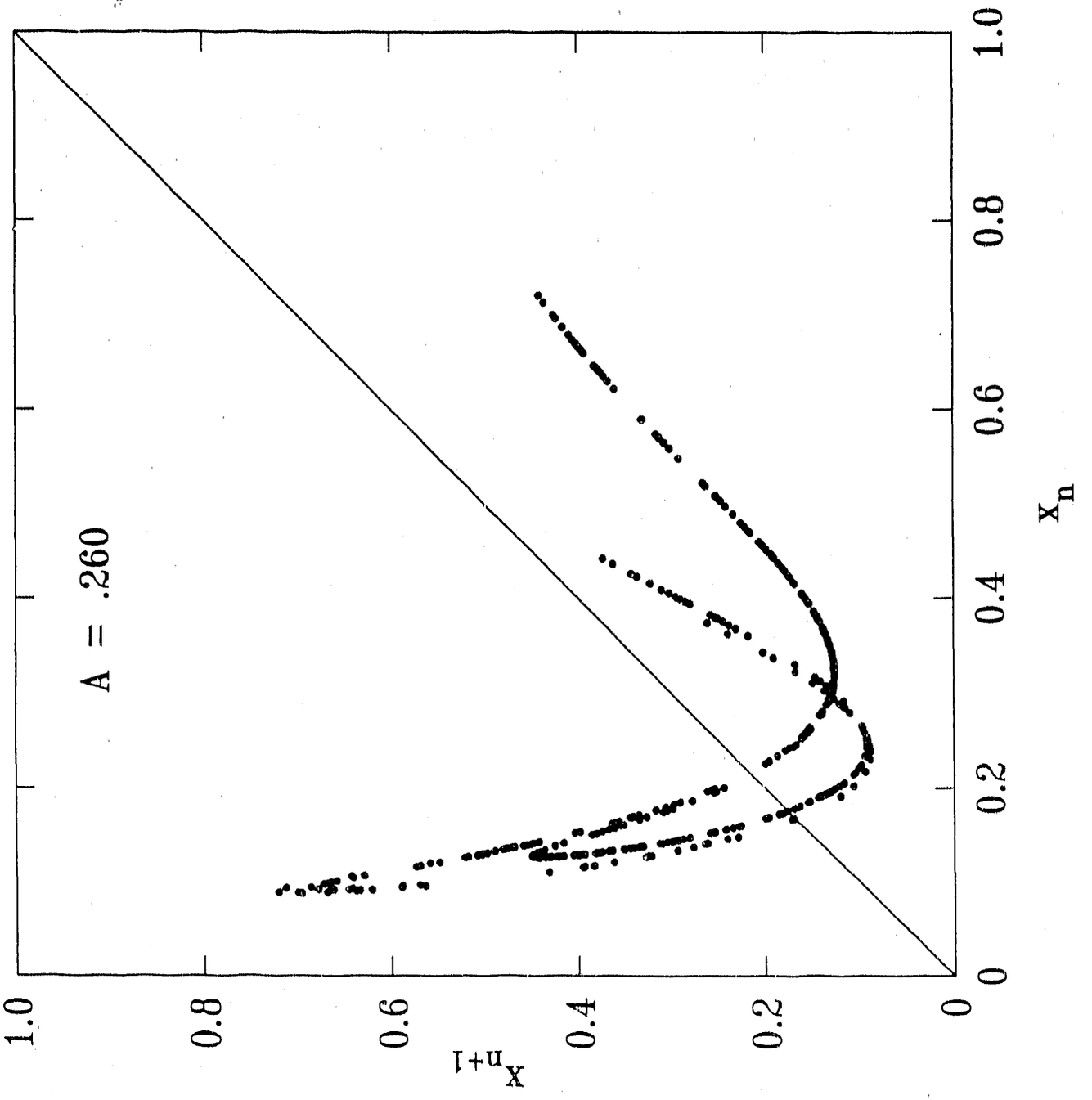

Fig. 6b

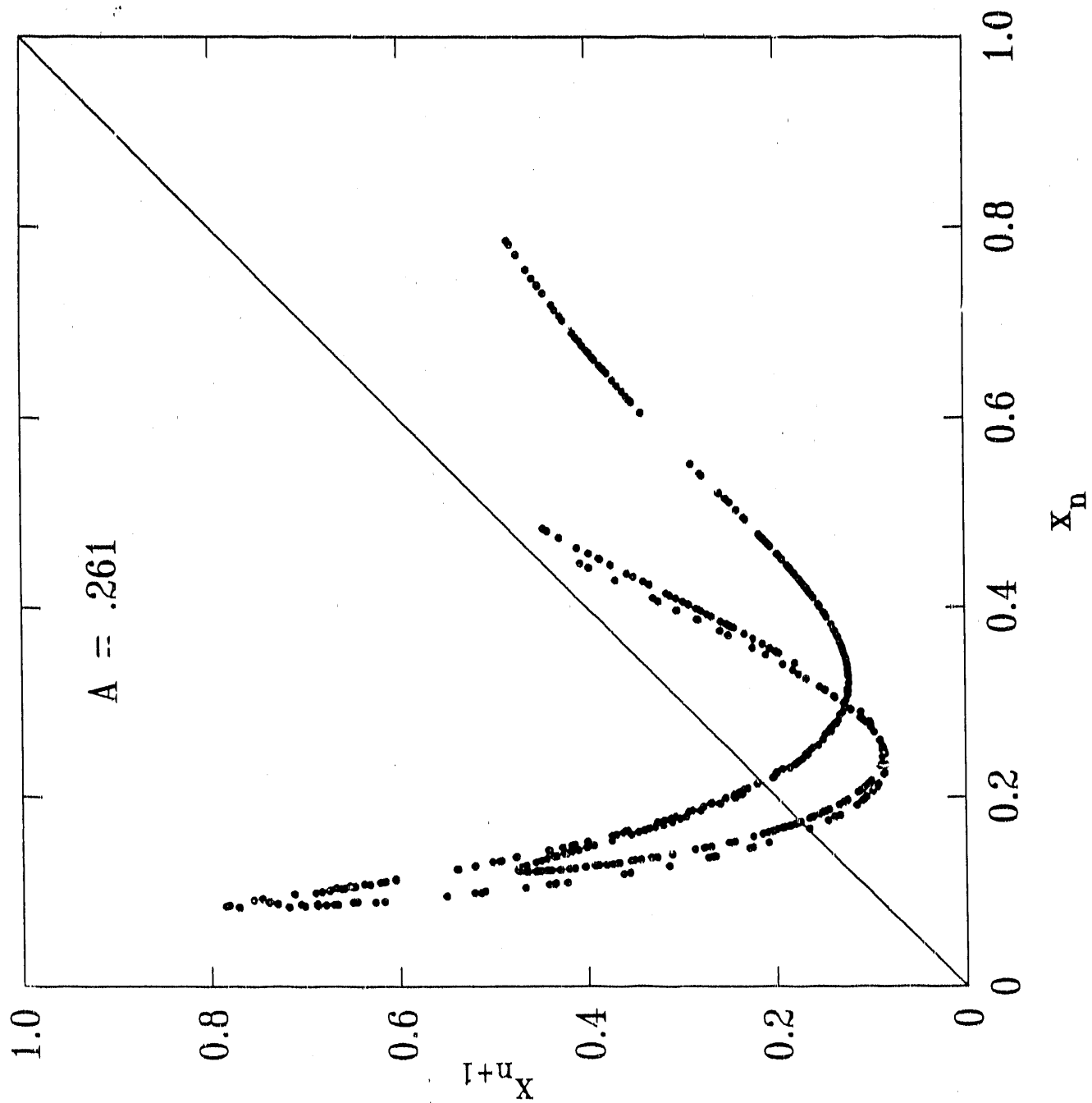

Fig. 6c

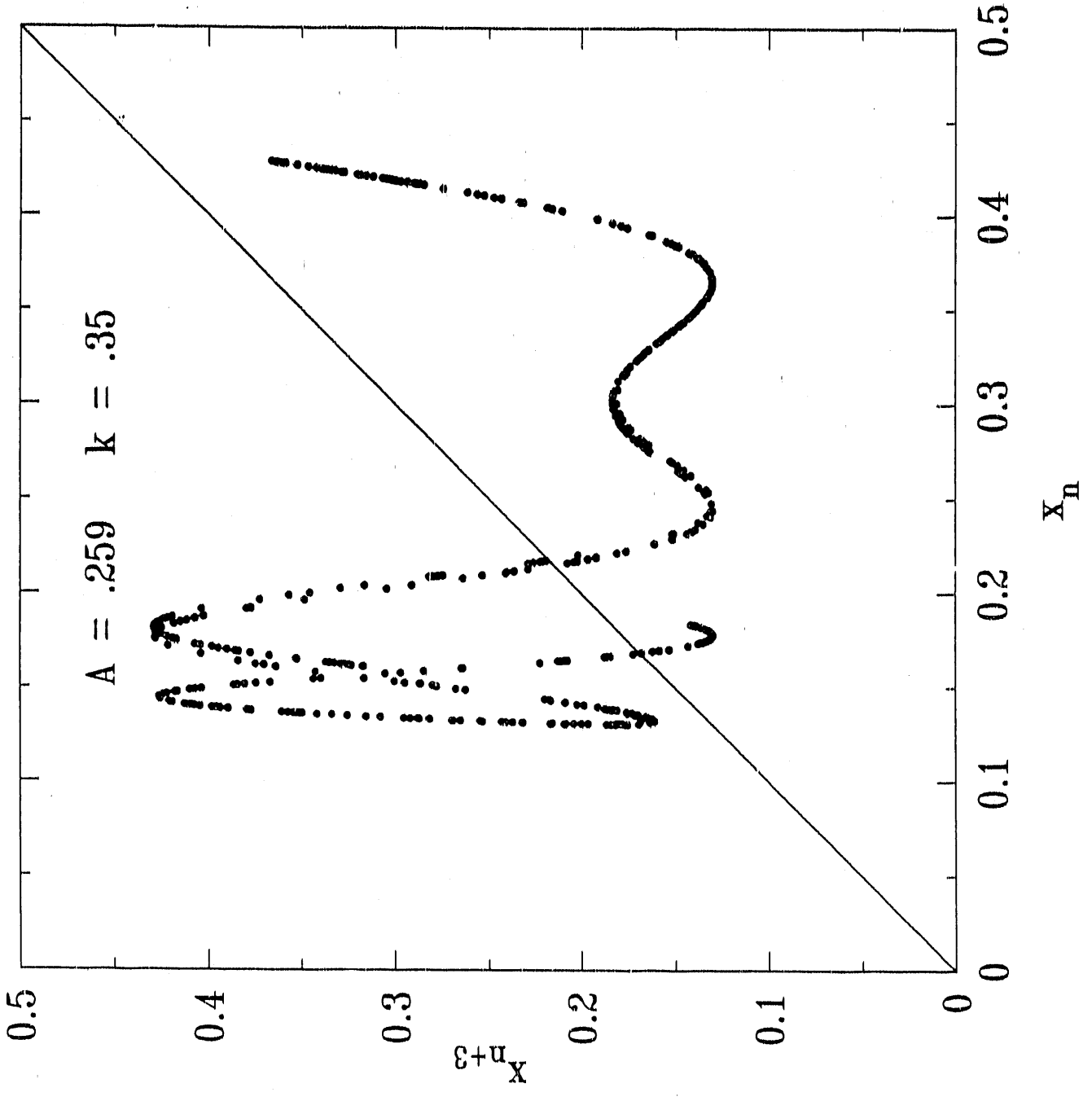

Fig. 6d

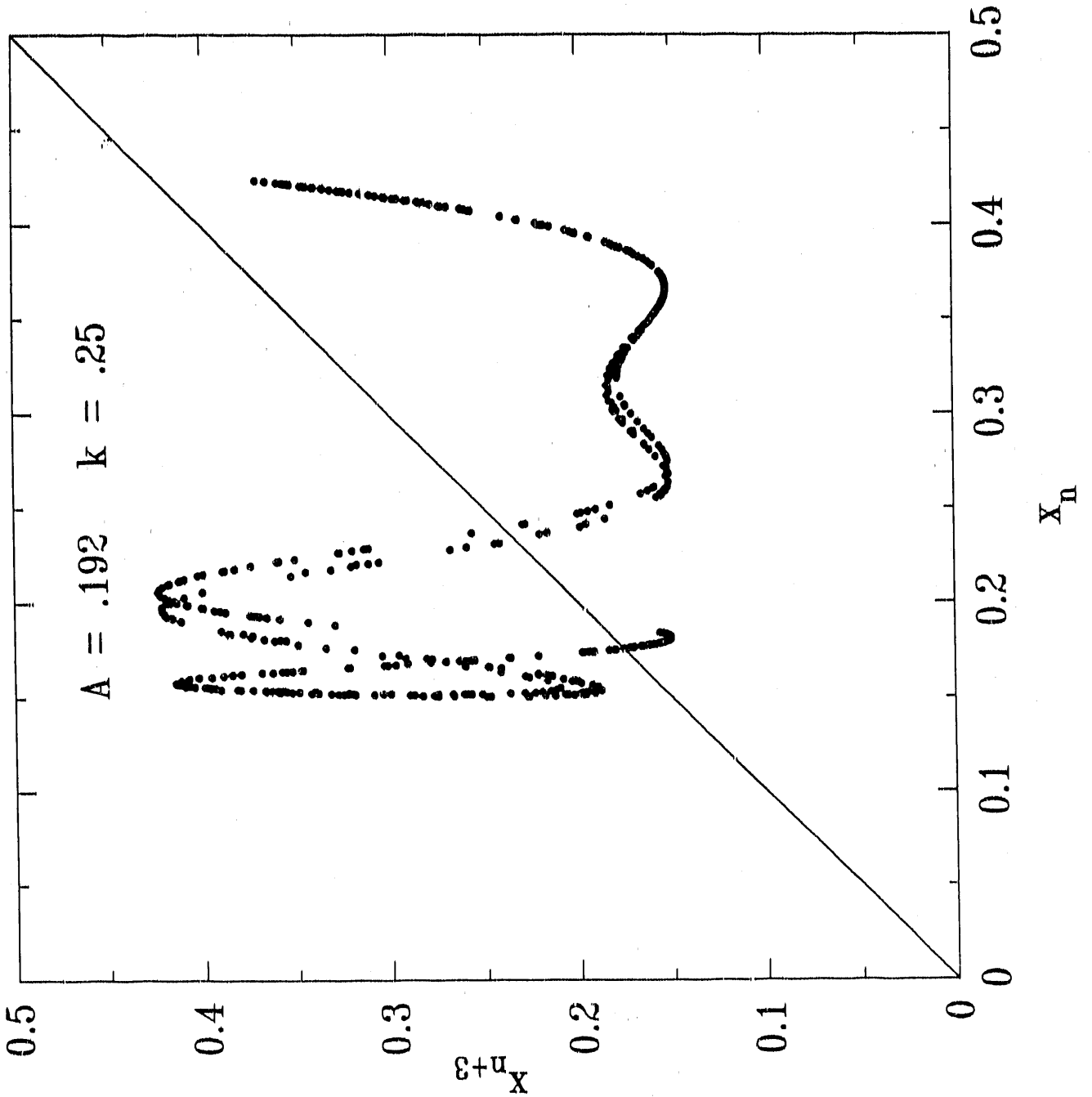

-END-

DATE FILMED

11 / 06 / 90